ARTICLE

doi:10.1038/nature16531

Structural disorder of monomeric α-synuclein persists in mammalian cells

Francois-Xavier Theillet[1]†*, Andres Binolfi[1]†*, Beata Bekei[1]*, Andrea Martorana[2], Honor May Rose[1], Marchel Stuiver[1], Silvia Verzini[1], Dorothea Lorenz[3], Marleen van Rossum[1], Daniella Goldfarb[2] & Philipp Selenko[1]

Intracellular aggregation of the human amyloid protein α-synuclein is causally linked to Parkinson's disease. While the isolated protein is intrinsically disordered, its native structure in mammalian cells is not known. Here we use nuclear magnetic resonance (NMR) and electron paramagnetic resonance (EPR) spectroscopy to derive atomic-resolution insights into the structure and dynamics of α-synuclein in different mammalian cell types. We show that the disordered nature of monomeric α-synuclein is stably preserved in non-neuronal and neuronal cells. Under physiological cell conditions, α-synuclein is amino-terminally acetylated and adopts conformations that are more compact than when in buffer, with residues of the aggregation-prone non-amyloid-β component (NAC) region shielded from exposure to the cytoplasm, which presumably counteracts spontaneous aggregation. These results establish that different types of crowded intracellular environments do not inherently promote α-synuclein oligomerization and, more generally, that intrinsic structural disorder is sustainable in mammalian cells.

The effect of the crowded intracellular environment on the structure and dynamics of proteins is poorly understood, which is particularly evident for proteins that lack folded structures in the absence of binding partners, that is, intrinsically disordered proteins (IDPs)[1]. Human α-synuclein (αSyn) is a prototypic IDP characterized by its role as the primary protein component of amyloid deposits (termed Lewy bodies) in the brains of patients with Parkinson's disease and other synucleinopathies[2]. While αSyn is abundantly expressed throughout the brain[3], amyloid aggregates are primarily found in remnants of apoptotic dopaminergic neurons of the substantia nigra[4]. This raises the possibility that αSyn adopts different structures in different types of neuronal cells and that these structures exhibit different aggregation propensities[5]. In this light, recent reports postulate that αSyn principally exists as a folded helical tetramer in intact prokaryotic and eukaryotic cells[6,7]. Although subsequently challenged in several follow-up studies[8–11], as well as progressively adjusted by the proponents of the initial hypothesis[12–14], the monomer–tetramer controversy remains central to ongoing discussions about the native structural state(s) of αSyn in mammalian cells[15]. Addressing this question is crucial for our understanding of possible mechanisms of amyloid formation, not only in the case of αSyn and Parkinson's disease, but also for the plethora of other neurodegenerative disorders involving IDPs[16].

αSyn is disordered in mammalian cells

To obtain atomic-resolution insights into the structure and dynamics of αSyn in mammalian cells, we performed in-cell NMR experiments in non-neuronal A2780 and HeLa cells, and neuronal B65, SK-N-SH and RCSN-3 cells, the latter being directly derived from rat substantia nigra neurons[17]. To generate in-cell NMR samples in the physiological concentration range of endogenous αSyn in primary neurons, that is, from 5 to 50 μM (refs 3, 18), we developed a simple electroporation protocol to deliver defined amounts of ^{15}N isotope-enriched αSyn into cultured mammalian cells (Fig. 1a). To ensure the physiological intactness of our in-cell NMR samples, we assessed cell viability by flow cytometry and used immunofluorescence and electron microscopy to establish that delivered αSyn distributed evenly throughout the cytoplasm of electroporated cells (Fig. 1b and Extended Data Fig. 1a, b). In line with previous findings, we measured an intracellular protein half-life of ~50 h (ref. 19) without significant changes in cytoplasmic αSyn staining (Fig. 1c). To correlate the effective NMR concentrations of isotope-enriched αSyn in the different cell samples with concentrations that we determined by semi-quantitative western blotting, we recorded one-dimensional (1D) ^{15}N-filtered in-cell NMR spectra on all specimens (Fig. 2a and Extended Data Fig. 1c). Amide-envelope intensity matching verified that 90 ± 10% (mean ± s.e.m.) of delivered αSyn molecules contributed to the measured in-cell NMR signals (S_{eff}), demonstrating that exogenously delivered αSyn tumbled freely in the cytoplasm of electroporated cells, and did not stably interact with large cellular structures such as membranes. Cell viability and leakage tests after in-cell NMR experiments ruled out signal contributions from external αSyn (Extended Data Fig. 1d, e).

Residue-resolved two-dimensional (2D) ^{1}H–^{15}N in-cell NMR spectra of αSyn in A2780, HeLa, RCSN-3, B65 and SK-N-SH cells displayed strong similarities with the disordered reference state of the isolated protein, with average backbone amide chemical shift changes ($\Delta\delta$) smaller than 0.01 p.p.m. (Fig. 2b and Extended Data Fig. 1f). These results showed that the different intracellular environments did not induce major conformational rearrangements of monomeric αSyn. We detected varying degrees of NMR signal broadening in the amino and carboxy terminus of αSyn, which were highly reproducible in replicate in-cell NMR samples (Extended Data Fig. 2).

[1]In-Cell NMR Laboratory, Department of NMR-supported Structural Biology, Leibniz Institute of Molecular Pharmacology (FMP Berlin), Robert-Rössle Strasse 10, 13125 Berlin, Germany. [2]Department of Chemical Physics, Weizmann Institute of Science, Rehovot 76100, Israel. [3]Department of Molecular Physiology and Cell Biology, Leibniz Institute of Molecular Pharmacology (FMP Berlin), Robert-Rössle Strasse 10, 13125 Berlin, Germany. †Present addresses: Department of Biochemistry, Biophysics and Structural Biology, Institute for Integrative Biology of the Cell (I2BC), UMR9198 CNRS, Bât 144, CEA Saclay, 91191 Gif-sur-Yvette, France (F.-X.T.); Max Planck Laboratory for Structural Biology, Chemistry and Molecular Biophysics of Rosario (MPLbioR-UNR) and Instituto de Investigaciones para el Descubrimiento de Fármacos de Rosario (IIDEFAR-CONICET), 27 de Febrero 210 bis; S2002LRK-Rosario, Argentina (A.B.).
*These authors contributed equally to this work.

© 2016 Macmillan Publishers Limited. All rights reserved

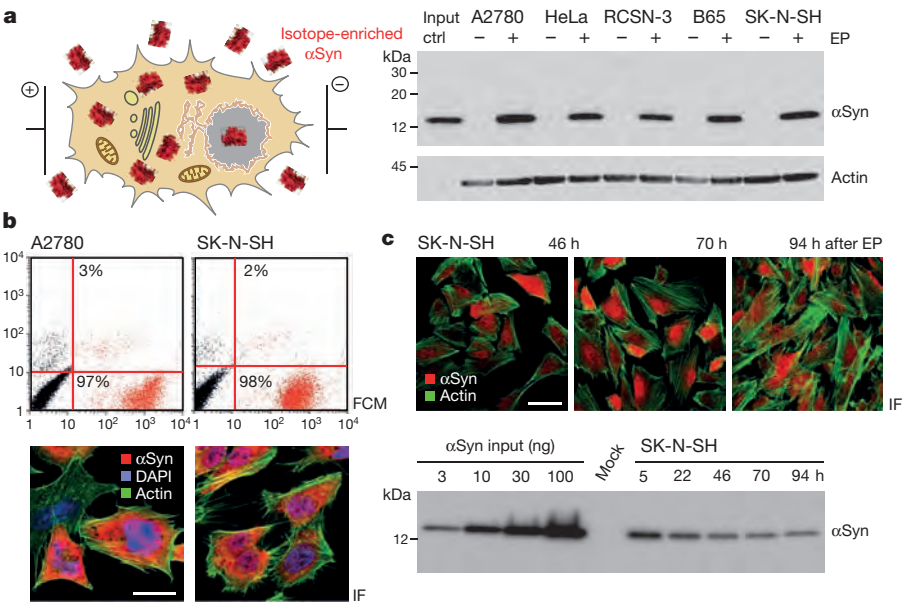

Figure 1 | Delivery of αSyn into mammalian cells. a, Electroporation of ^{15}N isotope-enriched αSyn into A2780, HeLa, RCSN-3, B65 and SK-N-SH cells delivers 'NMR-visible' protein into 'NMR-invisible' intracellular environments. Western blotting confirms comparable levels of αSyn transduction. Ctrl; control; EP, electroporated; kDa, kilodaltons. **b**, Top, flow cytometry (FCM) scatter plots of mock-electroporated (black) and Atto488-tagged αSyn-electroporated (red) A2780 and SK-N-SH cells. Percentages of viable αSyn-positive (bottom quadrant, *x* axis) and apoptotic 7-AAD-positive (top quadrant, *y* axis) cells are indicated. Bottom, immunofluorescence (IF) imaging of αSyn (red) in electroporated A2780 and SK-N-SH cells. Phalloidin staining shows actin filaments (green), DAPI staining identifies cell nuclei (blue). Scale bar, 20 μm. **c**, Immunofluorescence time course of αSyn localization and stability in SK-N-SH cells 46, 70 and 94 h after electroporation. αSyn dilution owing to cell division is compensated with higher laser power settings. Scale bar, 50 μm. Semi-quantitative western blotting of intracellular αSyn at indicated time points after electroporation (total number of electroporated cells loaded). Protein concentrations are determined based on a dilution series of recombinant αSyn. For gel source data, see Supplementary Fig. 1.

αSyn is N-terminally acetylated in cells

All in-cell NMR spectra exhibited reduced signal intensities of the first ten residues of αSyn with peak positions that closely matched those of the N-terminally acetylated protein (Fig. 2c and Extended Data Fig. 3a). Cell lysis obliterated the observed line-broadening effects and clearly revealed the spectral features of N-terminal acetylation (Extended Data Fig. 3b). In further support of the soluble nature of intracellular αSyn, we quantitatively recovered the monomeric protein in the cytoplasmic fractions of in-cell NMR sample lysates (Extended Data Fig. 3c). Having used electroporation to deliver recombinantly produced, non-acetylated αSyn into mammalian cells, we reasoned that N-terminal acetylation must have occurred post-translationally. This conclusion challenges the prevalent view that N-terminal acetylation of eukaryotic proteins is established in an exclusive co-translational manner, when nascent polypeptides exit the ribosome[20]. Our findings further confirm that N-terminally acetylated αSyn represents the physiological form of the protein, in line with previous reports[6,10]. As observed before, acetylation led to higher levels of residual helicity within the N terminus of αSyn[21,22] and to avid binding of small unilamellar vesicles (SUVs) that we reconstituted from pig brain polar lipids (Extended Data Fig. 4a, b). Irrespective of N-terminal acetylation, however, in-cell NMR experiments did not reveal the spectral features of fully membrane-associated αSyn, such as uniform signal broadening of its first ~100 residues[22,23], thus ruling out stable membrane interactions.

αSyn interacts with the cytoplasm

To characterize the dynamic properties of acetylated αSyn in the different intracellular environments, we measured in-cell NMR peak intensity changes and backbone amide relaxation parameters in A2780 and SK-N-SH cells (Extended Data Fig. 4c–e), and in artificially crowded solutions containing Ficoll, BSA, lysozyme, SUVs or urea (Extended Data Fig. 5). In cells, signal attenuations primarily affected N- and C-terminal αSyn residues, whereas a biologically inert crowding agent such as Ficoll did not recapitulate these line-broadening effects (Fig. 3a). The addition of BSA or lysozyme to N-terminally acetylated αSyn led to selective reductions of N- or C-terminal signal intensities, respectively, which were reminiscent of the observed in-cell NMR behaviour. Having obtained residue-resolved intracellular ^{15}N relaxation data (longitudinal (R_1), transverse (R_2) and ^{1}H–^{15}N hetero-nuclear Overhauser effect (NOE) values), we separated dynamic contributions on the fast nanosecond time scale governing the residue-specific rotational correlation time (τ_c) of αSyn, from effects in the micro- to millisecond time range giving rise to exchange terms (R_{ex}) that also reflect weak transient interactions with cytoplasmic components. Higher τ_c profiles reported a uniform decrease of αSyn dynamics in A2780 and SK-N-SH cells, and in the differently crowded *in vitro* environments as expected for viscosity-driven reductions in overall αSyn mobility[24] (Fig. 3b and Extended Data Fig. 6a). By contrast, we determined non-uniform exchange contributions in A2780 and SK-N-SH cells, which were largest for the first ten residues of αSyn and also affected amino acids around Tyr39 and the C terminus of the protein (Fig. 3c and Extended Data Fig. 6b). We detected similar N- or C-terminal exchange profiles with BSA (pI 4.7) or lysozyme (pI 11.35), respectively (Fig. 3c and Extended Data Fig. 6c, d). To test whether complementary electrostatic interactions with the partially charged N and C termini of αSyn gave rise to these effects, we increased the salt concentrations of BSA- and lysozyme-crowded solutions and re-determined R_{ex} contributions of αSyn. We observed no salt effects with BSA, whereas R_{ex} terms in lysozyme-crowded solutions decreased at higher salt concentrations (Fig. 3c and Extended Data Fig. 6e), suggesting that electrostatic interactions mediated the C-terminal exchange behaviour of αSyn. Suspecting alternative hydrophobic effects as the cause for exchange contributions in the N terminus of αSyn, we replaced Phe4 and Tyr39 with alanine residues (that is, F4A;Y39A) and re-measured protein dynamics and R_{ex} in A2780 and SK-N-SH cells, and in the presence of BSA (Fig. 3c and Extended Data Fig. 7a). We found diminished

© 2016 Macmillan Publishers Limited. All rights reserved

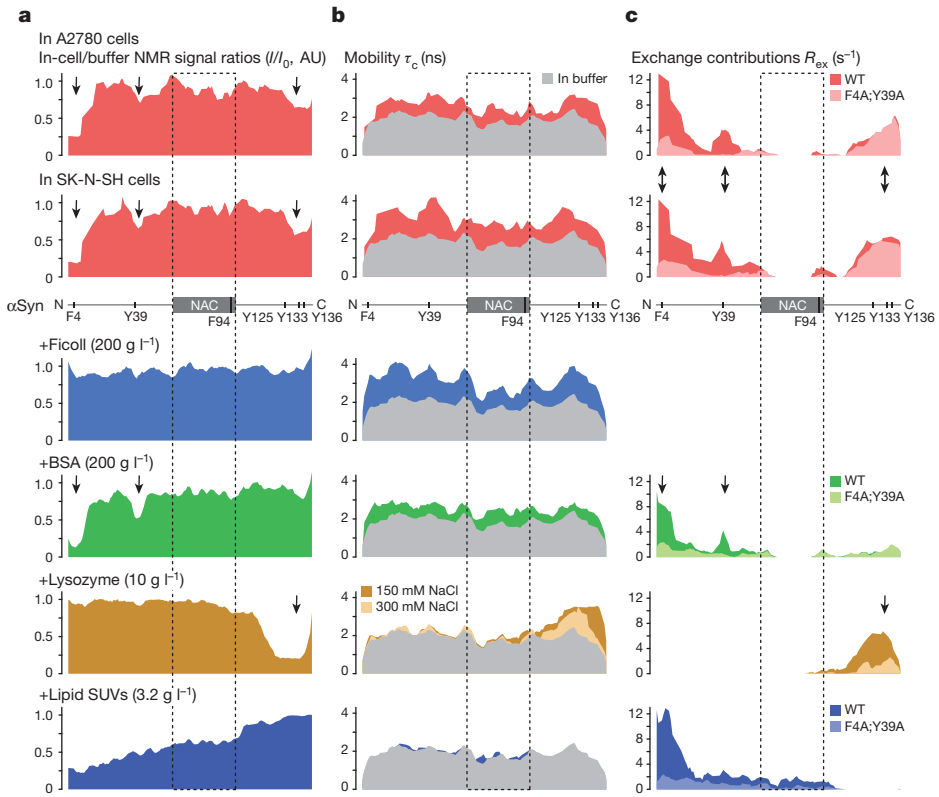

Figure 3 | αSyn dynamics in cells and crowded solutions. a, Residue-resolved NMR signal intensity ratios (I/I_0) of αSyn in A2780 and SK-N-SH cells (red) identify regions of site-selective line broadening (marked by arrows). No line broadening of N-terminally acetylated αSyn is observed in the presence of Ficoll (blue), whereas BSA (green) and lysozyme (orange) recapitulate signal attenuations of N- and C-terminal residues, respectively. Addition of sub-saturating amounts of SUVs to N-terminally acetylated αSyn leads to a gradual reduction of NMR signal intensities of its first 100 residues. For simplification, all profiles show values averaged over three consecutively resolved residues. AU, arbitrary units. **b**, Residue-resolved rotational correlation time (τ_c) of N-terminally acetylated αSyn in buffer (grey), in cells (red), and in the presence of different crowding agents (averaged over three consecutively resolved residues) reveal uniform reductions of fast protein motions. **c**, Site-specific exchange contributions (R_{ex}) identify αSyn regions that engage in weak transient interactions with cytoplasmic components (marked with arrows). Substitution of Phe4 and Tyr39 with alanine residues (F4A;Y39A) reduces N-terminal R_{ex} terms in cells (light red) and in BSA-crowded solutions (light green), thus identifying hydrophobic contacts as the source of N-terminal exchange contributions. Higher salt concentrations diminish C-terminal αSyn interactions with lysozyme (light orange), arguing for electrostatic effects. Different from BSA-crowded solutions, only residues 1–20 of N-terminally acetylated αSyn exhibit pronounced exchange contributions in the presence of sub-saturating amounts of SUVs (blue), which are diminished for αSyn(F4A;Y39A) (light blue).

that the protein exhibits transient long-range interactions between N- and C-terminal residues[27,28]. These intramolecular contacts result in loosely packed αSyn structures that deviate from extended polypeptide chain conformations and occlude the central NAC region. PRE experiments on Gd(III)-labelled αSyn in A2780 and SK-N-SH cells revealed distance profiles that were similar to those of the isolated protein, thus arguing for the preservation of intramolecular αSyn contacts in intact cells (Fig. 5a and Extended Data Fig. 8). Notably, however, in-cell PRE profiles also indicated greater levels of αSyn compaction, which suggested that both intracellular environments strengthen, rather than weaken, the structural features that αSyn displays in buffer. PRE experiments in Ficoll- and BSA-crowded solutions (200 g l^{-1}) recapitulated these compaction effects (Fig. 5b), whereas denaturation with 8 M urea led to extended αSyn structures (Extended Data Fig. 8). Complementary DEER experiments in A2780 cells confirmed these results (Extended Data Fig. 9c, d). To test whether αSyn formed oligomers or aggregates in A2780 cells, we also performed intermolecular DEER and PRE measurements[29]. Even at intracellular αSyn concentrations above 50 μM, neither experimental approach yielded indications for such events, although we detected sparsely populated αSyn oligomers in the presence of 200 g l^{-1} Ficoll and BSA (Extended Data Fig. 9e, f).

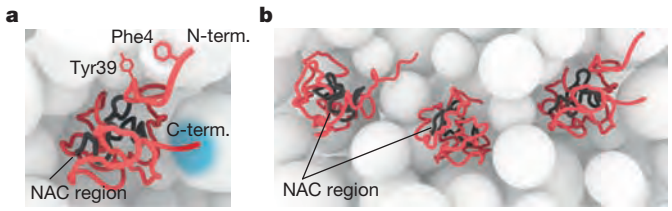

Figure 4 | αSyn interactions and conformations in cells. a, Cartoon representation of localized hydrophobic and electrostatic interactions of αSyn with cytoplasmic components, shown schematically as white spheres. Hydrophobic contacts are mediated by aromatic residues Phe4 and Tyr39 in the N terminus of αSyn whereas negatively charged residues in the C terminus engage in complementary electrostatic interactions with positively charged intracellular surfaces (indicated in blue). The central NAC region (dark grey) is shielded from exposure to the cytoplasm and does not interact with intracellular components. **b**, Cartoon models of possible ensemble conformations of monomeric αSyn in cells.

Discussion

Our results show that exogenously delivered αSyn exists as an N-terminally acetylated, disordered and highly dynamic monomer in neuronal and non-neuronal cells, without detectable signs of oligomerization, spontaneous aggregation, or targeted degradation. In the absence of chemical cross-linking[12–14] and the concomitant introduction of oligomer-promoting agents such as dimethyl sulfoxide (DMSO)[30], monomeric αSyn represents the predominant species in the cytoplasm of cells analysed in this study. Although we cannot

© 2016 Macmillan Publishers Limited. All rights reserved

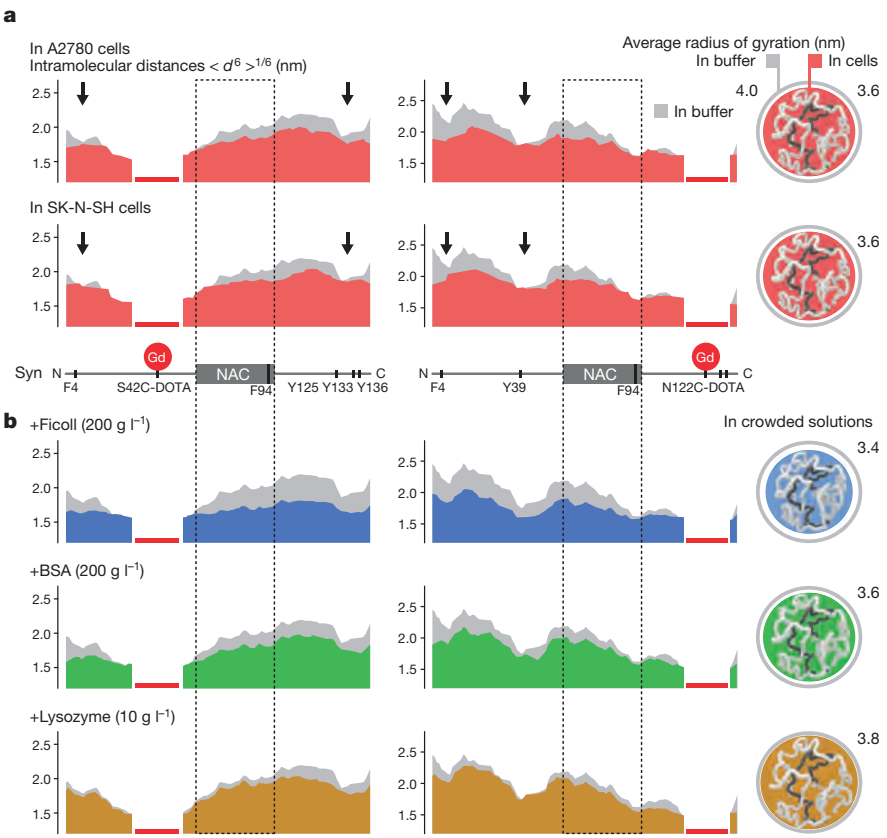

Figure 5 | Compact αSyn structures in cells and crowded solutions. **a**, Intramolecular PRE-derived distance profiles of N-terminally acetylated αSyn in buffer (grey) and in A2780 and SK-N-SH cells (red). **b**, Comparative PRE-derived distance profiles in Ficoll- (blue), BSA- (green) and lysozyme- (orange) crowded solutions. Gd(III)-DOTA tags at residues 42 (left; S42C-DOTA) and 122 (right; N122C-DOTA) provide complementary information about αSyn compaction in the respective environments. Proximal PRE effects render residues adjacent to the conjugated Gd(III) invisible (red bars). PRE-derived distances were obtained assuming that every Gd(III)-^{1}H vector fluctuation rate scales linearly with that of the backbone N–H vector and the Gd(III)-DOTA complex. For simplification, profiles show values averaged over three consecutively resolved residues. Comparisons of αSyn dimensions in buffer, in cells and in the presence of different crowding agents are shown on the right. Average radii of gyration and levels of αSyn compaction are delineated based on the scaling of representative PRE distances relative to values measured in buffer (see Supplementary Methods and Extended Data Fig. 8). In the depicted cartoon models, residues of the NAC region are coloured in dark grey. Arrows denote regions of marked intramolecular contacts.

rule out the presence of other lowly populated αSyn states in our in-cell NMR and EPR samples, we can exclude scenarios in which most αSyn molecules adopt stably folded, or fully membrane-associated structures[6,9]. In-cell conformations of αSyn are generally more compact than in buffer, and shield hydrophobic residues of the amyloidogenic NAC region from interactions with the cytoplasm, similar to the folding principle of structured proteins. By contrast, Phe4 and Tyr39 prominently engage in transient interactions with cytoplasmic components, whereas negatively charged residues in the αSyn C terminus participate in weak electrostatic contacts. Both types of interactions can be recapitulated in artificially crowded *in vitro* solutions and are lost after cell lysis, reminiscent of previously observed quinary structure interactions of folded and partially disordered proteins in prokaryotic and eukaryotic cells[31,32]. By exhibiting structural features that disfavour NAC-mediated interactions, large conformational rearrangements appear to be necessary for αSyn to oligomerize under native cell conditions[33], for which the identified sampling of hydrophobic contacts by Phe4 and Tyr39, including the transient binding of cellular membranes may set the stage[34]. Given that these residues are critical for αSyn aggregation *in vitro*[35], they may also constitute 'interaction hotspots' in the formation of early αSyn oligomers in cells.

Online Content Methods, along with any additional Extended Data display items and Source Data, are available in the online version of the paper; references unique to these sections appear only in the online paper.

Received 9 June; accepted 14 December 2015.
Published online 25 January 2016.

1. Theillet, F. X. *et al.* Physicochemical properties of cells and their effects on intrinsically disordered proteins (IDPs). *Chem. Rev.* **114,** 6661–6714 (2014).
2. Goedert, M., Spillantini, M. G., Del Tredici, K. & Braak, H. 100 years of Lewy pathology. *Nature Rev. Neurol.* **9,** 13–24 (2013).
3. Iwai, A. *et al.* The precursor protein of non-A beta component of Alzheimer's disease amyloid is a presynaptic protein of the central nervous system. *Neuron* **14,** 467–475 (1995).
4. Lashuel, H. A., Overk, C. R., Oueslati, A. & Masliah, E. The many faces of alpha-synuclein: from structure and toxicity to therapeutic target. *Nature Rev. Neurosci.* **14,** 38–48 (2013).
5. Dettmer, U., Selkoe, D. & Bartels, T. New insights into cellular α-synuclein homeostasis in health and disease. *Curr. Opin. Neurobiol.* **36,** 15–22 (2015).
6. Bartels, T., Choi, J. G. & Selkoe, D. J. α-Synuclein occurs physiologically as a helically folded tetramer that resists aggregation. *Nature* **477,** 107–110 (2011).
7. Wang, W. *et al.* A soluble α-synuclein construct forms a dynamic tetramer. *Proc. Natl Acad. Sci. USA* **108,** 17797–17802 (2011).
8. Binolfi, A., Theillet, F. X. & Selenko, P. Bacterial in-cell NMR of human alpha-synuclein: a disordered monomer by nature? *Biochem. Soc. Trans.* **40,** 950–954 (2012).
9. Burré, J. *et al.* Properties of native brain α-synuclein. *Nature* **498,** E4–E6 (2013).
10. Fauvet, B. *et al.* Characterization of semisynthetic and naturally N-alpha-acetylated α-synuclein *in vitro* and in intact cells: implications for aggregation and cellular properties of alpha-synuclein. *J. Biol. Chem.* **287,** 28243–28262 (2012).
11. Fauvet, B. *et al.* α-Synuclein in central nervous system and from erythrocytes, mammalian cells, and *Escherichia coli* exists predominantly as disordered monomer. *J. Biol. Chem.* **287,** 15345–15364 (2012).

© 2016 Macmillan Publishers Limited. All rights reserved

12. Dettmer, U., Newman, A. J., Luth, E. S., Bartels, T. & Selkoe, D. *In vivo* cross-linking reveals principally oligomeric forms of α-synuclein and β-synuclein in neurons and non-neural cells. *J. Biol. Chem.* **288,** 6371–6385 (2013).
13. Dettmer, U. *et al.* Parkinson-causing alpha-synuclein missense mutations shift native tetramers to monomers as a mechanism for disease initiation. *Nature Commun.* **6,** 7314 (2015).
14. Luth, E. S., Bartels, T., Dettmer, U., Kim, N. C. & Selkoe, D. J. Purification of α-synuclein from human brain reveals an instability of endogenous multimers as the protein approaches purity. *Biochemistry* **54,** 279–292 (2015).
15. Selkoe, D. *et al.* Defining the native state of α-synuclein. *Neurodegener. Dis.* **13,** 114–117 (2014).
16. Uversky, V. N. Intrinsically disordered proteins and their (disordered) proteomes in neurodegenerative disorders. *Front. Aging Neurosci.* **7,** 18 (2015).
17. Paris, I. *et al.* The catecholaminergic RCSN-3 cell line: a model to study dopamine metabolism. *Neurotox. Res.* **13,** 221–230 (2008).
18. Wilhelm, B. G. *et al.* Composition of isolated synaptic boutons reveals the amounts of vesicle trafficking proteins. *Science* **344,** 1023–1028 (2014).
19. Okochi, M. *et al.* Constitutive phosphorylation of the Parkinson's disease associated α-synuclein. *J. Biol. Chem.* **275,** 390–397 (2000).
20. Starheim, K. K., Gevaert, K. & Arnesen, T. Protein N-terminal acetyltransferases: when the start matters. *Trends Biochem. Sci.* **37,** 152–161 (2012).
21. Kang, L. *et al.* N-terminal acetylation of alpha-synuclein induces increased transient helical propensity and decreased aggregation rates in the intrinsically disordered monomer. *Protein Sci.* **21,** 911–917 (2012).
22. Maltsev, A. S., Ying, J. F. & Bax, A. Impact of N-terminal acetylation of α-synuclein on its random coil and lipid binding properties. *Biochemistry* **51,** 5004–5013 (2012).
23. Dikiy, I. & Eliezer, D. N-terminal acetylation stabilizes N-terminal helicity in lipid- and micelle-bound alpha-synuclein and increases its affinity for physiological membranes. *J. Biol. Chem.* **289,** 3652–3665 (2014).
24. Li, C. *et al.* Differential dynamical effects of macromolecular crowding on an intrinsically disordered protein and a globular protein: Implications for in-cell NMR spectroscopy. *J. Am. Chem. Soc.* **130,** 6310–6311 (2008).
25. Fusco, G. *et al.* Direct observation of the three regions in α-synuclein that determine its membrane-bound behaviour. *Nature Commun.* **5,** 3827 (2014).
26. Martorana, A. *et al.* Probing protein conformation in cells by EPR distance measurements using $Gd3^{+}$ spin labelling. *J. Am. Chem. Soc.* **136,** 13458–13465 (2014).
27. Bertoncini, C. W. *et al.* Release of long-range tertiary interactions potentiates aggregation of natively unstructured α-synuclein. *Proc. Natl Acad. Sci. USA* **102,** 1430–1435 (2005).
28. Dedmon, M. M., Lindorff-Larsen, K., Christodoulou, J., Vendruscolo, M. & Dobson, C. M. Mapping long-range interactions in α-synuclein using spin-label NMR and ensemble molecular dynamics simulations. *J. Am. Chem. Soc.* **127,** 476–477 (2005).
29. Wu, K. P. & Baum, J. Detection of transient interchain interactions in the intrinsically disordered protein α-synuclein by NMR paramagnetic relaxation enhancement. *J. Am. Chem. Soc.* **132,** 5546–5547 (2010).
30. Kostka, M. *et al.* Single particle characterization of iron-induced pore-forming α-synuclein oligomers. *J. Biol. Chem.* **283,** 10992–11003 (2008).
31. Danielsson, J. *et al.* Thermodynamics of protein destabilization in live cells. *Proc. Natl Acad. Sci. USA* **112,** 12402–12407 (2015).
32. Monteith, W. B., Cohen, R. D., Smith, A. E., Guzman-Cisneros, E. & Pielak, G. J. Quinary structure modulates protein stability in cells. *Proc. Natl Acad. Sci. USA* **112,** 1739–1742 (2015).
33. Cremades, N. *et al.* Direct observation of the interconversion of normal and toxic forms of α-synuclein. *Cell* **149,** 1048–1059 (2012).
34. Galvagnion, C. *et al.* Lipid vesicles trigger α-synuclein aggregation by stimulating primary nucleation. *Nature Chem. Biol.* **11,** 229–234 (2015).
35. Lamberto, G. R. *et al.* Structural and mechanistic basis behind the inhibitory interaction of PcTS on α-synuclein amyloid fibril formation. *Proc. Natl Acad. Sci. USA* **106,** 21057–21062 (2009).
36. Ulmer, T. S. & Bax, A. Comparison of structure and dynamics of micellebound human α-synuclein and Parkinson disease variants. *J. Biol. Chem.* **280,** 43179–43187 (2005).

Supplementary Information is available in the online version of the paper.

Acknowledgements We thank J. Burre, T. Sudhof, D. Jovin, D. Mulvihill, P. Caviedes and T. Maritzen for plasmids and reagents, and for critical discussions. V. Subramanian, D. Eliezer, J. Clark and J. Dyson for carefully reading the manuscript and helpful comments. M. Herzig for essential input in the development of the electroporation protocol and M. Beerbaum and P. Schmieder for maintenance of the NMR infrastructure. RCSN-3 cells are made available by P. Caviedes upon request (pcaviede@med.uchile.cl). F.-X.T. acknowledges funding from the Association pour la Recherche sur le Cancer (ARC). D.G. acknowledges support by the Israel Science Foundation (ISF) F.I.R.S.T. program (grant 1114/12). P.S. was funded by the Deutsche Forschungsgemeinschaft (DFG) via an Emmy Noether Project Grant (SE1794/1-1). This work is supported by the European Research Council (ERC) Consolidator Grant (CoG) 'NeuroInCellNMR' (647474) awarded to P.S.

Author Contributions F.-X.T. and A.B. performed in-cell and *in vitro* NMR experiments. B.B., H.M.R., S.V., M.v.R. and M.S. developed the electroporation protocol, manipulated and handled cells, and performed light microscopy, cell and molecular biology experiments. A.M. and D.G. designed and performed EPR experiments, and analysed data. D.L. performed electron microscopy experiments. F.-X.T., A.B. and P.S. conceived the study, analysed the data and wrote the paper. F.-X.T., A.B. and B.B. contributed equally. All authors discussed the results and commented on the manuscript.

Author Information Reprints and permissions information is available at www.nature.com/reprints. The authors declare no competing financial interests. Readers are welcome to comment on the online version of the paper. Correspondence and requests for materials should be addressed to P.S. (selenko@fmp-berlin.de).

© 2016 Macmillan Publishers Limited. All rights reserved